Journal of Scientific & Industrial Research
Vol. 81, September 2022, pp. 922-931
DOI: 10.56042/jsir.v81i09.52645

Mathematical Modelling of a Box Type Solar Cooker Incorporating Contact Resistance

H. A. Vaidya*[1,2] & S. A. Channiwala[2]

[1]Government Engineering College, Surat, Gujarat, India 395 007

[2]Sardar Vallabhbhai National Institute of Technology, Surat, Gujarat, India 395 007

Received 20 July 2021; revised 18 August 2022; accepted 25 August 2022

A solar cooker is a device that uses solar energy to heat food to cook it. Solar cooking is used to reduce conventional fuel usage and improve the quality of food. Solar cookers have to deal with high concentration heat flows through the contact between metal parts of the absorber plate and the food vessel. For heat transfer, thermal contact resistance plays an important role and it is a major concern to reduce the thermal resistance at the contact. In the present work, mathematical modeling of a lightweight, energy-efficient box-type solar cooker is done by incorporating contact resistance. An experimental setup is developed to find out the thermal contact resistance and thermal contact resistance is evaluated for surface roughness of 0.2 Ra and 0.8 Ra for the Aluminum material. Performance tests of the cooker are carried out to get the figure of merits F_1 and F_2. Also, the load test with the measured thermal contact resistance is carried out with surface roughness of 0.8 and 0.2 Ra. For surface roughness of 0.2 Ra, the % error is observed as 19.77%, 13.69%, 13.68% considering thermal resistance at joints, and −42.89%, 18.95%, and 16.37% without considering thermal resistance at joints. For surface roughness of 0.8 Ra, the deviation is observed as 23.09%, 17.52%, 13.5% considering thermal resistance at joints and −42.89%, 18.95% and16.37% without considering thermal resistance at joints. The figure of merit F_1 is calculated as 0.12 as compared to 0.11 for the commercial cookers, which shows that the newly designed cooker has higher optical efficiency. The figure of merit F_2 is calculated as 0.42 against 0.38 for the commercial cookers. The results thus emphasize that thermal contact resistance is important and should be considered during modeling.

Keywords: Heat transfer, Metals, Performance test, Surface roughness

Introduction

For the better part of the past few decades, natural gas has been a fuel that is both very affordable and very readily available for use in the kitchen and heating water. However, as a result of the depletion of natural fossil reserves, there is a growing demand for alternative fuels that, in due course of time, are capable of substituting for natural gas. Electricity can be prohibitively expensive or nonexistent in some more rural areas. Solar cookers offer an uncomplicated and cost-effective method of cooking for households that are looking for ways to save money.

In the work that is being presented here, mathematical modeling of box-type solar cookers is carried out with the incorporation of contact resistance. This model can be used to find out the time required to get the food cooked. Various researchers have carried out experiments on solar cookers for their performance and analysis. Amongst all forms of solar cookers, a box-type solar cooker is the simplest. Researchers have given different designs and evaluated their performances. In their study, various researchers have focussed on studying the effects of parameters affecting the performance of solar cookers like glazing, type, the number of reflectors[1], variations in load and, number of pots.[2],variables that are controllable like solar insolation catching area, overall heat transfer coefficient and thermal conductivity of absorber plate and variables that cannot be controlled such as solar radiation, temperature variance and load dispersal[3], roughness element geometries[4],natural heat transfer coefficient[5] and weight analysis.[6] Many researchers derived and presented correlations for measurements of top loss coefficient[7] and equation based on simple thermal investigations on trapezoidal absorber plate of the form $Nu = CRa^{n5}$

Many researchers have given the mathematical model for the analysis of the solar cooker of various designs. Harmim *et al.*[8] proposed a new design where

*Author for Correspondence
E-mail: hemish2000@gmail.com

the cooking pot is indirectly getting the solar radiation with an irregular complex parabolic concentrator as a reflector which focuses solar fallout captured on horizontal orifice towards vertical absorber plate and established a mathematical model for it. Pejack[9] established a mathematical model and obtained approximate factors for various conditions predicting solar cooker performance. Terres *et al.*[10] proposed a mathematical model to determine heat transfer on box-type solar cookers having internal reflectors and validated by experimental and simulation results. Das *et al.*[11] proposed a mathematical model for the heat transfer process in solar cooker by varying parameters like the thickness of the plate, vessel emissivity, the thickness of insulation and its effect on cooking time has been studied. They suggested that avoiding the use of black paint on vessels is possible if vessels made of weathered stainless steel or aluminium are utilised instead. El sebaii[12] presented an unsteady mathematical model for a box-type solar cooker with one step outward reflector pivoted at the top of the cooker by comparing their temperature profile with their experimental observations. Many researchers have also tried to study the effect of thermal contact resistance between solid surfaces. Nikolic and lukic[13] introduced a mathematical model for determining the optimal reflector position in a double exposure collector so that the lower absorber surface receives full irradiation. The use of a flat-plate reflector that is placed underneath and parallels the collector allows for absorption to occur on the lower surface of the absorber.

Yovanovich *et.al.*[14] concentrated on solids having both surfaces rough and wavy. The impact of different parameters on resistance at contact in vacuum conditions was contemplated. They proposed the hypothesis that two surfaces united under load, really contact at disconnected miniaturized scale contacts, and the subsequent genuine zone is the aggregate of these smaller-scale contacts. Liu *et al.*[15] prepared a simple test setup at room temperature and conducted experiments on brass columns by varying interfacial pressure, voltage, environmental temperature compensation and thermally conductive adhesive. The thermal resistance at joints was found lower with temperature compensation and with the use of thermally conductive adhesive and almost constant with an increase in input voltage.

Khounsary *et al*[16] studied the effect of interface pressure on thermal contact conductance on copper-silicon contact in vacuum conditions with different interface materials like foil of Indium, foil of Silver, and a liquid eutectic (Ga-In-Sn). The thermal conductance at the joint increased with an increase in interstitial pressure except for eutectic in which it was found to be constant. The minimal thermal resistance at joints across the Cu-Si edge was found in liquid metal, Indium foil and then silver foil respectively. Tomimura *et al.*[17] explored the key factors for the inconsistencies among measured thermal resistance at joints, even for similar materials. For this, they carried out an analysis using a simple contact surface approach, which was made up of a unit cell model by Tachibana and Sanokawa and Hertzian contact model. The proposed assessment equations for flat rough surfaces and wavy rough surfaces and attempted experimentally to affirm with sets of the cylindrical brass specimen.

Shylkov and Ganin[18] proposed a condition and technique to compute thermal resistance between two diverse metal surfaces with various loads and finishes. They demonstrated that thermal resistance at joints diminishes with more pressure on surfaces in contact. To start with this reduction is sharp, and after that, it progresses toward becoming smoother. They likewise demonstrated that thermal resistance at joints declines with increment in temperature. The tests were performed in reducing chamber pressures which demonstrated that thermal resistance at joints gets increment when atmospheric pressure diminishes. Lee *et al.*[19] studied the performance of interface materials like sheets of graphite oil, a sheet of silicone, a sheet of fluoro ether oil, and synthetic grease in microelectronics packing usage and equated the results with bare surfaces. The variation in the contact pressure was 10 to 50 psi as any pressure more than 50 psi may damage the packing itself. They concluded that the data taken at high contact pressure are irrelevant in microelectronics packing uses. The measured results at low compressions are nearly three times the published values. Merrill & Garimella[20] performed experimental and numerical analysis, and concluded that the base material's effect on the coating material's effect on resistance at the contact is dependent on the base material, and that the layer thickness required for the lowest contact resistance varies greatly depending on the base material, surface finish, and surface coating. Heat transfer resistance can occur when the coating oxidizes or when the coating itself is very porous. The selection of the

coating material, the coating thickness, and even, on occasion, the properties of the base metal and its metrology are the fundamental design factors in the majority of applications. Regardless of whether or not there is a coating present, the roughness of the surface, the thermal conductivity, and the hardness of the base material are all very important factors.

Mikic[21] studied various theories of heat conductance at the contact of minutely levelled surfaces and expressed that the method of deformation significantly influenced the estimation of conductance. Conditions for thermal conductance were determined for (1) Pure plastic disfigurement (2) plastic twisting and versatile distortion of the base metal and (3) Pure elastic disfigurement. It was discovered that the primary factor for thermal resistance at joints in pure plastic disfigurement is asperities, in the plastic stream are RMS estimation of the surface roughness (σ) and the normal slope of the severities, and in pure elastic disfigurement, just surface roughness (σ) is an essential part. Wolff and Schneider[22] the effects of pressure, the hardness of the specimen, the surface roughness and the thermal properties of the interstitial material were studied as they related to the thermal resistance among two smooth steel substrates. It was more important that the border material be able to bond to the base material's surface materials than for the material to have good conductivity. When compared to the conductance of metallic foils like indium or annealed copper, the conductance of a heat sink compound based on silicone and paint filled with silver was significantly higher. The conductance was found to be higher after the temperature had been raised. This trend was most noticeable in the Teflon tape, copper and indium foils, and Teflon foils that were subjected to lower pressures. Stewart[23] performed an experimental and analytical investigation to determine the thermal resistance at joints of several metal specimen pairs using a pulse technique. He determined that thermal resistance at joints decreases by increasing the interface contact pressure. The microscopic surface irregularities will deform thereby increasing the actual contact area between the two specimens. Mikic and Rohsenow[24] developed prediction methods of the thermal resistance at joints for various surface features under the following cases: (i) rough planes that are supposedly flat, contained within a vacuum; (ii) rough planes that are supposedly flat and are in an environment with fluid; (iii) smooth wavy planes in a vacuum condition (with any of the following waviness involved; spherical waviness, single direction cylindrical waviness or perpendicular directional cylindrical waviness) and (iv) rough wavy surfaces in a vacuum conditions. They also derived an equation to find thermal contact resistance.

Macmillan and Mikic[25] considered the impact of unevenness and waviness on interstitial pressure and contact resistance. They came to the conclusion that the contact conductance of wavy surfaces could be increased for certain ranges of parameters if the surfaces were made uneven. The thermal resistance among two solid bodies in contact with one another in a vacuum was taken into consideration by Cooper *et al.*[26] To predict the conductance of various contacts conveyed at the interface, both previously conducted tests and the results of electrolytically straight forward tests were taken into consideration. They illustrated that the parameters necessary to anticipate thermal exchange can be governed by a straightforward control of the mean profiles of the mating surface, in conjunction with an estimate derived from the distortion hypothesis. This allowed them to predict thermal exchange with high accuracy. The procedure relied more substantially on the dissemination of a couple of high peak positions of the surfaces. Rather than using a Gaussian distribution, it is proposed to make use of describing functions. These speculations were subjected to a couple of tests, and the results of those tests, along with the predictions made by these individuals, were analysed and compared.

From the review of literature, it is observed that many researchers[1–6] have worked on performance parameters of various solar cooker designs, many researchers[8–13] have worked on developing a mathematical model for different designs of solar cookers and many researchers[14–26] have worked on the contact resistance but very none have considered the effect of thermal contact resistance between the vessel and the absorber plate in the solar cooker, which plays a crucial role in the heat transfer process between them. Therefore, a mathematical model has been developed incorporating thermal contact resistance and it is applied to the developed light weight low-cost solar cooker in the present work.

Materials and Methods

For the experimentation work, a solar cooker with a double glass cover was developed to measure the performance under load and no-load conditions. The details are as below:

Fabrication of Solar Cooker

After achieving the optimal combination of materials to be used for the solar cooker, complete fabrication of the box type solar cooker has been carried out and is described in the subsequent text in a stepwise manner.

Absorber Tray

For the absorber, an Aluminium plate of dimensions 340 × 340 mm^2 i.e., 0.1156 m^2 of area and height of 70 mm is required. The dimension of the base is 340 × 340 mm^2 and the top dimension of the plate is 460 × 460 mm^2. The aluminium absorber plate is cut and bent inappropriate manner to achieve these dimensions. Surface preparation: It is prepared by removal of the dust and impurities by polishing, buffing and chemical cleaning. After preparing the absorber tray black matt paint is applied to the surface. On the bottom of the absorber plate, ceramic paint has been applied to reduce the bottom losses.

Housing and Cover System

For the outer body frame dimension 500 × 500 mm^2, the ACP panel is taken to make a box of the desired dimension.

For the insulation, glass wool (k=0.0484, ρ=32 kg/m^3) is used. An aluminium frame is used with proper dimensions. After making groove space in the frame, both inner and outer glass is fitted by using glue and are left for 5–6 hours for complete sticking. The absorber tray is fixed above another frame fitted inside the housing body. Glass frame is joined with the housing body with the help of a hinge. At last, one handle on the top frame and one hook in the housing body are attached by a screw in such a way that after the opening of the top frame sufficient opening remains for keeping and removal of the cooking pot before and after cooking operation.

Instrumentation

For the solar cooker developed, T type thermocouples are used to measure the temperature at various locations with the help of a data logger. The solar radiations are measured by a class II Pyranometer and a data logger attached to it.

Selection, Calibration and Fixing of Thermocouples.

Type T thermocouples are chosen for their high sensitivity of 40-50 mV/°C. The following equation gives the relation among both temperature gradient and emf for iron constantan:

$$emf = C_1(T_1 - T_r) - C_2(T_2 - T_r) \quad \ldots (1)$$

where, C_1 and C_2 are constants.

T= Measuring junction temperature

T_r = Reference (cold) junction temperature

Thermocouple is calibrated with its reference junction at the ice point.

To measure mean temperature of plate, temperature of glass cover, internal air temperature and temperature of cooking food/water, 32 T type thermocouples are used. The location details of thermocouples are as under:

Absorber plate top-05, absorber plate bottom-02, outside glass top-02, outside glass-bottom-02, inside glass top-02, inside glass-bottom-02, sidewalls inside-04, side walls outside-04, thermocouples between the glass cover-02, pots-04, air mass-02 and ambient-01.

Mathematical Modeling

After the development of the solar cooker, modelling of the box-type solar cooker is done with a simple model without food utensils. Then the second level model is developed after considering useful heat gain from the top and bottom of the food vessel considering thermal contact resistance.

Solar Cooker Without Food Utensils

Aschematic diagram of the solar cooker without food utensils is shown in Fig. 1, the useful heat gained by the solar cooker can be found by the difference between the total heat gained by the solar cooker and the total heat loss from the solar cooker as per Sukhatme.[27]

Total heat gain can be calculated as the product of Solar flux and the Area of the absorber plate. Total heat loss is calculated as the product of overall heat loss coefficient, area of absorber plate and difference between mean plate temperature and ambient temperature

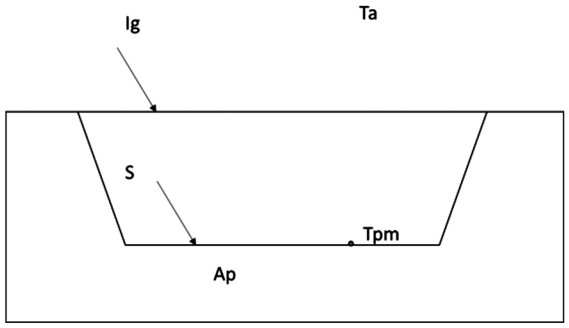

Fig. 1 — Schematic diagram of Solar Cooker without food utensil

Thus, the Useful heat gained by the absorber plate

$$Qu = SA_p – U_L A_p(Tpm – Ta) \quad \ldots (2)$$

Overall heat loss coefficient U_L can be calculated as

$$U_L = U_t + U_b + U_s$$

U_t is the top loss coefficient and is calculated as per Channiwala's correlation [7]

U_b and U_s are the bottom loss coefficient and side loss coefficient and are calculated as per Sukhatme[27]

Second Level Model

When a food utensil is kept in the cooker the food in the utensil receives heat from the lid by direct absorption of solar flux and from the bottom through thermal contact conductance. Hence a more versatile model is developed considering the useful heat gained by the food utensil from the top and the bottom. The schematic diagram of the second-level model is shown in Fig. 2.

From the basic concepts of heat transfer, considering transient heat conduction, the heat transferred to the food can be given by

$$Q_{uf} = M_f C_{pf} . \frac{dT_f}{dt} \quad \ldots (3)$$

Neglecting Evaporation and assuming U_L to be constant,

Useful heat gained by the food is the summation of heat gained from the top by solar flux and the heat gained from the bottom by the absorber plate minus the heat losses.

$$Q_{uf} = Q_t + Q \quad \ldots (4)$$

Useful heat gained from the top can be given by

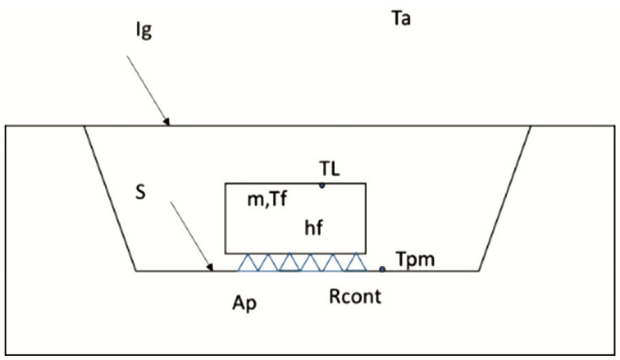

Fig. 2 — Solar cooker with food utensil considering thermal contact resistance (second level model)

$$Q_{t,u} = S.A_f – U_L.A_f(T_L – T_a) \quad \ldots (5)$$

where, $U_L.A_f$ $(T_L – T_a)$ is the heat loss from the lid of the vessel.

Useful heat gained from the bottom can be given by

$$Q_{b,u} = X.A_f.S – U_L.X.A_f(T_{pm} – T_a) \quad \ldots (6)$$

Assuming U_L to be constant and $X = \left(\frac{A_p}{A_f} – 1\right)$

where, $U_L.X.A_f$ $(T_{pm} – T_a)$ is the heat loss from the absorber plate.

Further algebraic calculations are continued in the Appendix I

Finally,

$$\mathbf{M_f . c_{pf} \frac{dT_f}{dt}} = X_{14}.\mathbf{S} – X_{15}.(T_f + X_{17}.T_a) \quad \mathbf{\ldots (7)}$$

where, $X_{17} = \frac{X_{16}}{X_{15}}$

Thus, by knowing the initial values of temperature of food, ambient temperature, Mass of food and specific heat of food, we can find the change in temperature of food with respect to time and thus we can also find the temperature of food (T_f) for a given period.

The heat transfer conductance h_{ct} is measured by experiments done on aluminium at surface roughness of 0.8 and 0.2. The details are given in the experimentation section. The heat transfer through food is calculated by the properties obtained at measured food temperature. Nusselt number is calculated by equation

$$Nu = 0.59 \times (Gr \times Pr)^{0.25} \quad \ldots (8)$$

and

$$h_f = Nu \times K / Lc \quad \ldots (9)$$

Experimentation

Experimentation on Solar Cooker

A set of experiments have been conducted on a fully instrumented optimized solar cooker as developed earlier, to measure the performance under load and no-load conditions. The figure of merit F_1 and Figure of merit F_2 has been calculated by

following equations for the developed cooker and both the figures of merit are compared with that of the commercial cooker.

$$F_1 = \frac{T_{pm}-T_a}{I_G} \quad \ldots (10)$$

and

$$F_2 = \frac{F_1(MC)_W}{A(t_2-t_1)}\ X\ ln\left\{\frac{1-\left(\frac{1}{F_1}\right)\left[\frac{T_{W2}-T_a}{I_G}\right]}{1-\left(\frac{1}{F_1}\right)\left[\frac{T_{W1}-T_a}{I_G}\right]}\right\} \quad \ldots (11)$$

Experiments were carried on 15-5-17, 17-7-17 and 19-7-17 for no-load tests and F_1 has been calculated. Load tests were carried out on 18-5-17, 20-5-17 and 23-5-17 and the figure of merit F_2 has been calculated. Developed solar cooker and commercial solar cooker are shown in Fig. 3.

A mathematical model has been developed for a box-type solar cooker with the incorporation of thermal resistance at joints as described in the section above and the results obtained by it are compared with the experimental results.

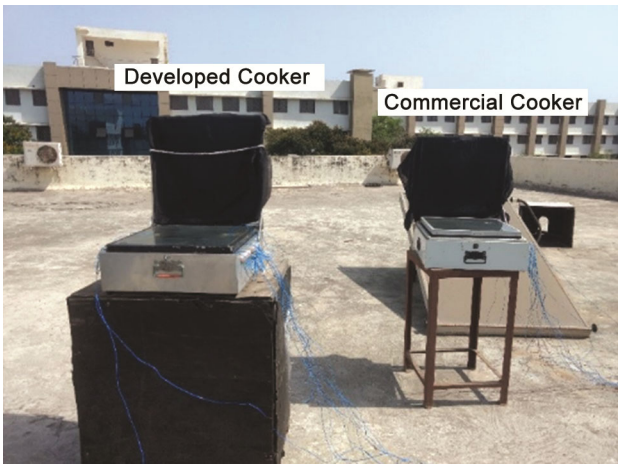

Fig. 3 — Developed and Commercial solar cooker

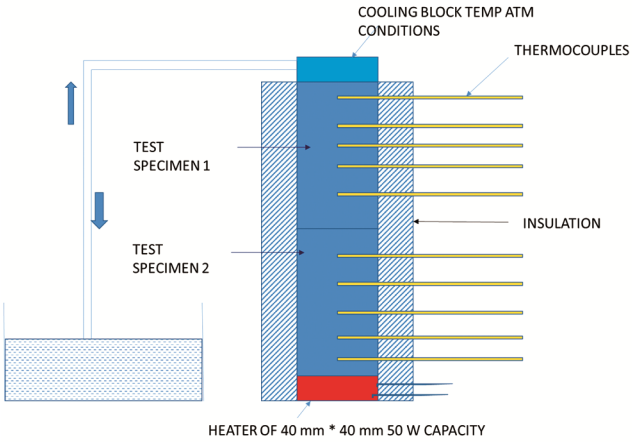

Fig. 4 — Schematic diagram of the experimental set-up

Experimentation for Thermal Contact Resistance

An experimental setup is developed to evaluate the thermal resistance at joints of metals of different surface roughness. The details of this set-up are given in subsequent sections:

Experimental Set Up for Measuring Thermal Contact Resistance

The schematic diagram of the experimental setup is shown in Fig. 4. The experimental setup, as shown in Fig. 5, consists of an electrical heater, a variac for voltage variation, a cooling water pump, two test specimens of Aluminium, a loading mechanism with pressure gauge, thermocouples, multimeter, and Cerawool for insulation etc.

Two test samples of 40 × 40 mm are kept on the heater. Ten thermocouples are fixed in the holes of the test sample. On the top of the test sample is the water-cooling system. Cerawool is used as the insulating material. It is covered around the two test samples along the side surfaces to stop the heat transmission in the lateral direction. The power of the electrical heater is adjusted by a variac. The power is changed from 15 to 75 watts during the trials. Interstitial pressure can be progressively changed by the hydraulic mechanism, which is applied to the test sample and the pressure is measured by the pressure

Fig. 5 — Experimental set-up

gauge on the apparatus. The sizes of the test sample are 40 × 40 mm square and 60 mm long.

Before the test, the contact planes are polished and surface roughness is estimated with Mitutoyo Surf test 210. Five holes were drilled on the test sample at 10 mm space and their dimensions are 4 mm in diameter and 20 mm deep. 5 K type thermocouples were introduced into each hole to measure the temperature dispersal in the test sample. The thermocouple indications were measured by a multimeter and the millivolts are converted into temperature. The temperature gradient in the test sample could be computed. With a known thermal conductivity of the material, and the temperature slope according to Fourier's law, the heat exchange rate can be figured as underneath

$$q = -k\frac{dT}{dx} \quad \ldots (12)$$

The temperatures obtained from the five thermocouples are extrapolated to the contact surface and the temperature difference obtained from the values of both specimens is calculated. The thermal resistance at joints can be calculated by dividing the temperature difference by the heat transferred.

$$R_{th} = \Delta T/q \quad \ldots (13)$$

Experimental Studies on Surface Roughness of 0.2 Ra and 0.8 Ra

Experimental investigations were carried out on Aluminium specimens for low and high surface roughness as 0.2 Ra and 0.8 Ra respectively. The power was varied from 15 to 75 watts and the interstitial pressure was kept at 0 MPa to simulate actual cooker conditions.

Result and Discussion

Results of Thermal Contact Resistance

Temperature variation with distance of thermocouples from the heater for Aluminum bars having surface roughness of 0.8 Ra at interstitial pressure of 0 MPa at voltage inputs of 15V, 18 V, 21 V and 24 V are shown in Fig. 6. The temperature distribution is found linear in both top and bottom specimens and a temperature difference is observed on extrapolating the temperature profile at the contact point due to thermal resistance at joints. It is also observed that temperature difference ΔT decreases with an increase in voltages at the same interstitial pressure.

Temperature variation with distance of thermocouples from the heater for Aluminum bars having surface roughness of 0.2 Ra at interstitial pressure of 0 MPa at voltage inputs of 15V, 18 V, 21 V and 24 V are shown in Fig. 7. The temperature distribution is found linear in both top and bottom specimens and a temperature difference are observed on extrapolating the temperature profile at the contact point due to thermal resistance at joints. It is also observed that temperature difference ΔT decreases with an increase in voltages at the same interstitial pressure.

Comparison of thermal resistance at joints of Aluminium at 0.8 Ra and 0.2 Ra is shown in Fig. 8. At 0.8 Ra, the thermal resistance at joints seems to decrease initially till 17 V, remains constant till 21 V and increases after 21 V. At 0.2 Ra, the thermal

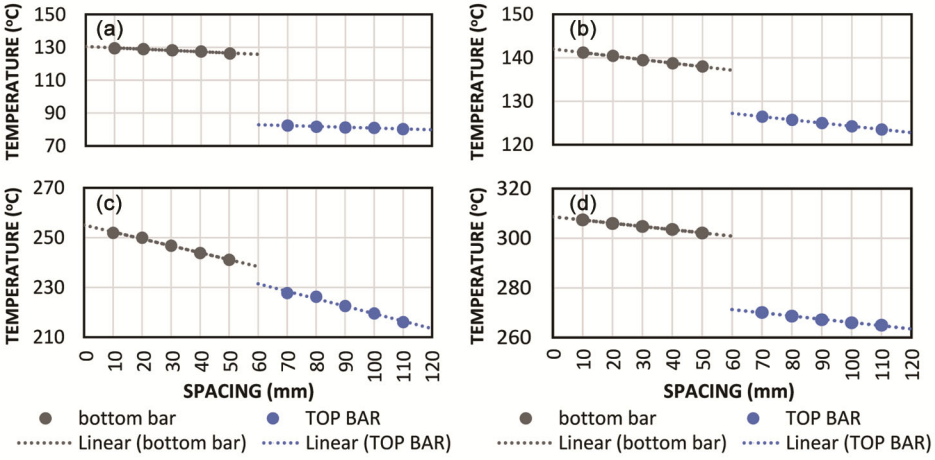

Fig. 6 — Variation of temperature at a different distance from heater for Aluminium at 0.8 Ra and 0 MPa interstitial Pressure at 15v, 18V, 21V and 24V

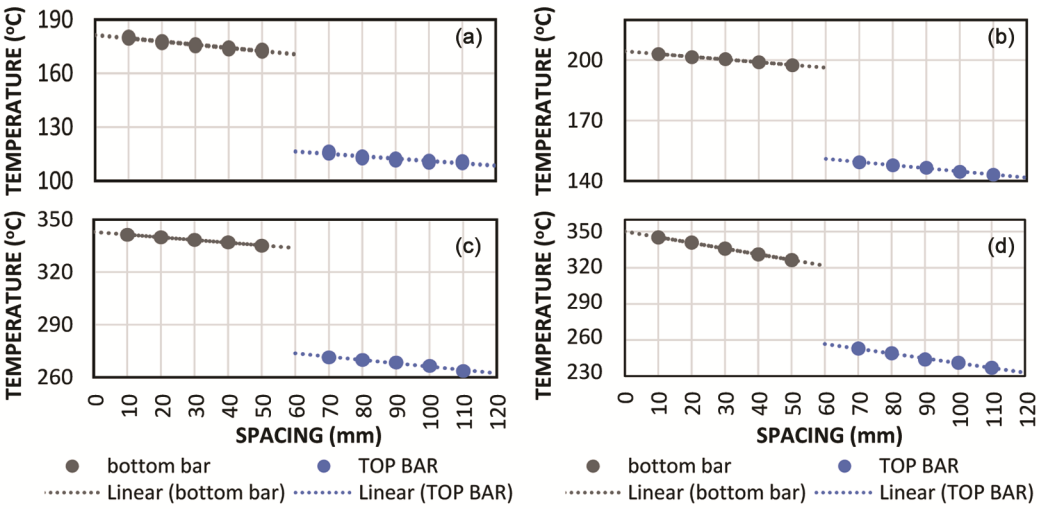

Fig. 7 — Variation of temperature at a different distance from heater for Aluminum at 0.2 Ra and 0 MPa interstitial Pressure at 15V, 18V, 21V and 24 V

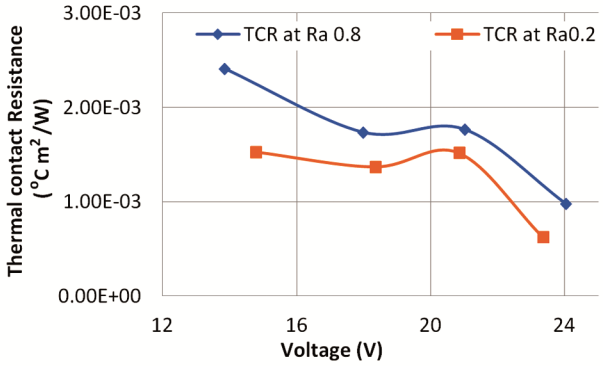

Fig. 8 — Comparison of Thermal Contact Resistance at Surface Roughness of 0.8 Ra and 0.2 Ra

resistance at joints remains constant at all voltages. The average value of thermal contact resistance for 0.8 Ra is found to be 1.73×10^{-3} and that for 0.2 Ra is found to be 1.26×10^{-3}. Thermal resistance at joints is observed less at surface roughness of 0.2 Ra than that at surface roughness of 0.8 Ra which is due to the reduced air gap between two surfaces.

Comparison of Thermal contact resistances obtained at surface roughness of 0.8 Ra by correlations of different researchers is done with that of experimental values in Table 1.

The values of TCR in experimental results are found to be much lower than that obtained from correlation of Serilee but of higher value than that obtained from Shylkov, Popov and Callaghan. Also wide variation in values of thermal contact resistances are obtained in experimental values and that predicted using published correlations. This focuses towards the need for more exhaustive experimental studies and come out with a better predictive tool for thermal contact resistances.

Table 1 — TCR at surface Roughness of 0.8 Ra

Interstitial Pressure	1MPa	2 MPa	3 MPa
TCR Expt	5.42×10^{-4}	3.82×10^{-4}	1.08×10^{-4}
TCR Serilee[19]	1.46×10^{-3}	7.56×10^{-4}	5.14×10^{-4}
TCR Shlykov[28]	3.30×10^{-7}	1.64×10^{-7}	1.09×10^{-7}
TCR Popov[29]	5.70×10^{-6}	2.94×10^{-6}	1.99×10^{-6}
TCR Callaghan[30]	2.09×10^{-7}	1.32×10^{-7}	1.01×10^{-7}

Results of Solar Cooker Tests

Following results are obtained during the load test for the solar cooker and the same are compared with the results obtained from the mathematical model developed incorporating the thermal resistance at contacts between the food vessel and the absorber plate.

Variation of water temperature considering the 0.2 Ra roughness value of pot on 20th May, 21st May and 23rd May 2017 is shown in Fig. 9.

The water temperature is found to be increasing with time in both experimental and modelled values in all three graphs. It is obvious due to the storage of heat in the solar cooker. Both the curves are found to be very nearly matching between 10 am to 1.00 pm. This suggests that the modelled value is quite appropriate to the experimental value. At about 1.00 pm both the values coincide showing that the evaporation of water has been reached and hence the experimental value will not rise beyond that temperature.

Variation of water temperature considering the 0.8 Ra roughness value of the Aluminum pot is shown in

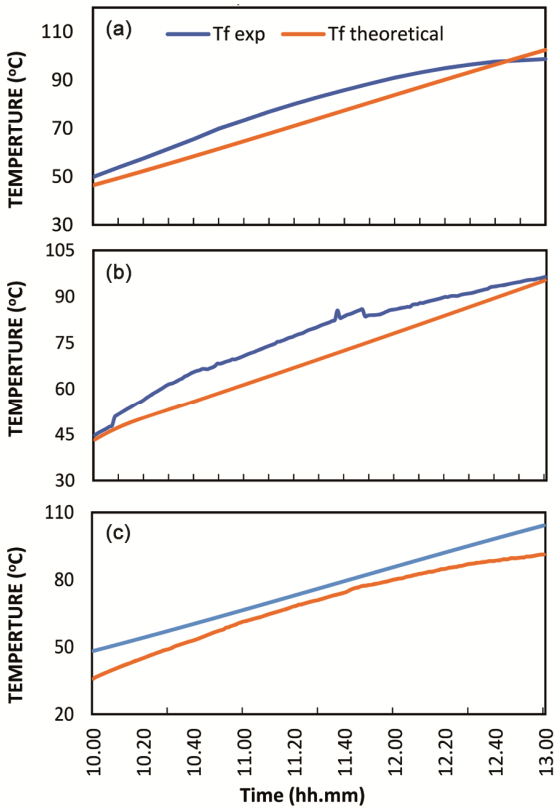

Fig. 9 — Variation of water temperature considering 0.2 Ra roughness of Aluminium Pot on 20th, 21st, and 23rd May 2017

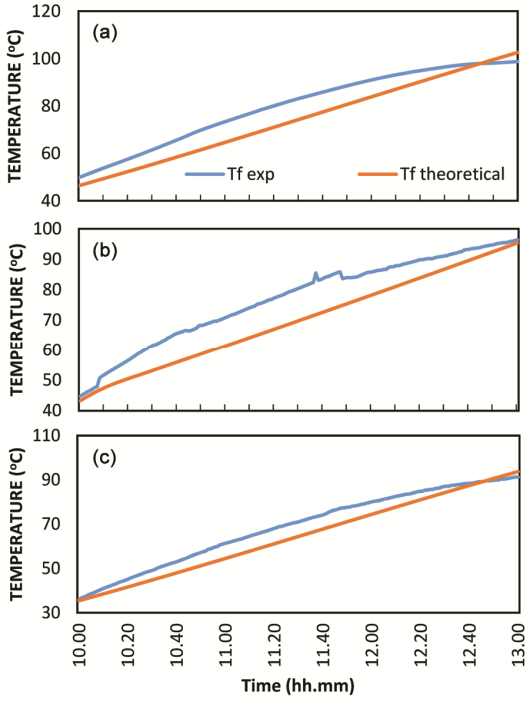

Fig. 10 — Variation of water temperature considering 0.8 Ra roughness of Aluminium Pot on 20th, 21st, and 23rd May 2017

Fig. 10. The water temperature is found to be increasing with time in both experimental and modelled values in all the three graphs, similar to Fig 9. In Fig 10, the difference observed in the experimental and modelled values are again found to be more than that in Fig 9. As the higher roughness value of 0.8 is considered, the conduction of heat between the absorber plate and the water in the pots is less due to more thermal resistance at joints. Thus, the thermal resistance at joints is the factor that cannot be neglected in the calculations of heat transfer from the absorber plate to the pot. The figure of merit F_1 calculated for the developed solar cooker was found to be 0.12 as compared to 0.11 for the commercial cookers. The figure of merit F_2 calculated for the developed solar cooker was found to be 0.42 as compared to 0.38 for the commercial cookers which proves the supremacy of the newly designed cooker over the commercial cooker.

Conclusions

The salient features of the present work can be summarized as follows:

The food temperature calculated in the model of the solar cooker by incorporating the thermal resistance at joints closely agrees with the experimental results. For surface roughness of 0.2 Ra, the % error is observed as 19.77%, 13.69%, 13.68% considering thermal resistance at joints and −42.89%, 18.95% and 16.37% without considering thermal resistance at joints. For surface roughness of 0.8 Ra, the deviation is observed as 23.09%, 17.52%, 13.5% considering thermal resistance at joints and −42.89%,18.95% and16.37% without considering thermal resistance at joints. The % error observed for 0.2 Ra considering thermal resistance at joints between 10.00 am to 1.00 pm is −9.36%, −12.06%, and 9.6%, and the % error observed for 0.8 Ra considering thermal resistance at joints between 10.00 am to 1.00 m is −7.51%, −9.7% and 9.4%.

There is a need of more comprehensive tool to predict thermal contact resistance.

The figure of merit F_1 = 0.12 as compared to 0.11 for the commercial cookers, which shows that the newly designed cooker has higher optical efficiency. The figure of merit F_2 = 0.42 against 0.38 of the commercial cookers.

Acknowledgement

The authors wish to express their gratitude to the administrative authorities of Sardar Vallabhbhai Patel National

Institute of Technology, Surat for providing the facilities to perform the experimental work.

Nomenclature

S Solar flux (W/m^2)

I_G Insolation on the horizontal surface at the time the stagnation temperature is reached(W/m^2)

A_p Aperture area of plate (m^2)

T_a Ambient temperature (°C)

T_{pm} Absorber plate mean temperature (°C)

Q_u Useful heat gain (W)

Q_{uf} Useful heat gain by food (W)

T_f Food temperature (°C)

T_L Temperature of the lid of food vessel(°C)

M_f Mass of food (kg)

C_{pf} specific heat of food in a vessel (kJ/kg°C)

A_f Area of food vessel (m^2)

h_{ct} Thermal Contact Conductance

U_L Overall loss coefficient

U_t Top loss coefficient

U_b Bottom loss coefficient

U_s Side loss coefficient

Q_t Heat gained by food from top

Q_b Heat gained by food from the bottom

F_1 Figure of Merit 1 from the stagnation test

F_2 Figure of Merit 2 from the load test

References

1 Mehta S & Channiwala S A, Comparative study of solar cookers, *Proc Nat Solar Energy Convention*, (Tata McGraw Hill Publishing Company Limited, New Delhi) Published online 1988, pp. 118–124.

2 Mullick S C, Kandpal T C & Kumar S, Testing of box-type solar cooker: second figure of merit F2 and its variation with load and number of pots, *Sol Energy*, **57(5)** (Published online 1996) 409–413.

3 Funk P A & Larson D L, Parametric model of solar cooker performance. *Sol Energy*, **62(1)** (1998) 63–68.

4 Gawande V B, Dhoble A S & Zodpe D B, Effect of roughness geometries on heat transfer enhancement in solar thermal systems — a review, *Renew Sustain Energy Rev*, **32** (2014) 347–378.

5 Kumar S, Natural convective heat transfer in trapezoidal enclosure of box-type solar cooker, *Renew Energy*, **29(2)** (2004) 211–222.

6 Goswami V, Harijan H, Pargi S, Pal S C, Vaidya H & Channiwala S, Analysis, design and performance evaluation of a light weight, energy efficient solar cooker, in *Int Conf Energy, Environ Econ*, 16th -18th August 2016, Heriot-Watt University, Edinburgh United Kingdom, 2016

7 Channiwala S A & Doshi N I, Heat loss coefficients for box-type solar cookers, *Sol Energy*, **42(6)** (1989) 495–501.

8 Harmim A, Merzouk M, Boukar M & Amar M, Performance study of a box-type solar cooker employing an asymmetric compound parabolic concentrator, *Energy*, **47(1)** (2012) 471–480.

9 Pejack E R, Mathematical model of the thermal performance of box-type solar cookers, *Renew Energy*, **1(5)** (1991) 609–615.

10 Terres H, Lizardi A, López R, Vaca M & Chávez S, Mathematical model to study solar cookers box-type with internal reflectors, *Energy Procedia*, **57** (2014) 1583–1592.

11 Das T C T, Karmakar S & Rao D P, Solar box-cooker: Part I—Modeling, *Sol Energy*, **52(3)** (1994) 265–272.

12 El-Sebaii A A, Domański R & Jaworski M, Experimental and theoretical investigation of a box-type solar cooker with multi-step inner reflectors, *Energy*, **19(10)** (1994) 1011–1021.

13 Nikolić N & Lukić N, A mathematical model for determining the optimal reflector position of a double exposure flat-plate solar collector, *Renew energy*, **51** (2013) 292–301.

14 Yovanovich M M & Rohsenow W M, *Influence of Surface Roughness and Waviness upon Thermal Contact Resistance*, Cambridge, Mass.: MIT Dept. of Mechanical Engineering, (1967), pp. 1–180.

15 Liu J, Feng H, Luo X, Hu R & Liu S, A simple setup to test thermal contact resistance between interfaces of two contacted solid materials, *Proc 11th Int Conf Electron Packag Technol High Dens Packag*, *ICEPT-HDP 2010*, 2010. doi:10.1109/ICEPT.2010.5582472

16 Khounsary A M, Chojnowski D, Assoufid L & Worek W M, Thermal contact resistance across a copper-silicon interface, in *High Heat Flux and Synchrotron Radiation Beamlines*, edited by A T Macrander, A M Khounsary, (SPIE) 1997, 45–51. doi:10.1117/12.294497

17 Tomimura T, Takahashi Y, Do T W, Shigyo K & Koito Y, Simple evaluation method for temperature drop at contact interface between rough surfaces under low contact pressure conditions. in *IOP Conf Ser: Mater Sci Eng* **Vol 61** (2014) 12040.

18 Shlykov Y P & Ganin Y A, Thermal resistance of metallic contacts, *Int J Heat Mass Transf*, **7(8)** (1964) 921–929.

19 Lee S, Early M & Pellilo M, Thermal interface material performance in microelectronics packaging applications, *Microelectronics J*, **28(1)** (1997), xiii–xx.

20 Merrill C T & Garimella S V, Measurement and prediction of thermal contact resistance across coated joints, *Exp Heat Transf*, **24(2)** (2011) 179–200.

21 Mikić B B, Thermal contact conductance; theoretical considerations, *Int J Heat Mass Transf*, **17(2)** (1974) 205–214.

22 Wolff E G & Schneider D A, Prediction of thermal contact resistance between polished surfaces, *Int J Heat Mass Transf*, **41(22)** (1998) 3469–3482.

23 Stewart Jr W E, Determination of thermal contact resistance between metals using a pulse technique, in *Symposium on Thermophysical Properties*, 6th, Atlanta, Ga, (Published online 1972), 1973, pp. 313–320.

24 Mikic B B & Rohsenow W M, *Thermal Contact Resistance*, Cambridge, Mass.: MIT Dept. of Mechanical Engineering, 1966, 1-95, doi:10.1007/BF01487469 M4 - Citavi

25 McMillan R & Mikic B B, *Thermal Contact Resistance with Non-Uniform Interface Pressures*, Cambridge, Mass.: MIT Engineering Projects Laboratory, 1970, 1-99.

26 Cooper M G, Mikic B B & Yovanovich M M, Thermal contact conductance, *Int J Heat Mass Transf*, **12(3)** (1969) 279–300.

27 Sukhatme S P & Nayak J K, *Solar Energy* (McGraw-Hill Education) 2017.

28 Shlykov Y P & Ganin Y A, Thermal resistance of metallic contacts, *Int J Heat Mass Transf*, **7(8)** (1964) 921–929. doi:10.1016/0017-9310(64)90147-4

29 Popov V M, Generalized relations for determining thermal contact resistance, *J Eng Phys*, **33(1)** (1977) 810–812, doi:10.1007/BF00861420

30 O'Callaghan P W & Probertt S D, "Thermal resistance and directional index of pressed contacts between smooth non-wavy surfaces." *J Mech Eng Sci* **16(1)** (1974) 41–55